HAL
open science

Disc fragmentation and the formation of Population III stars

M. A. Latif, D. R. G. Schleicher

▶ **To cite this version:**

M. A. Latif, D. R. G. Schleicher. Disc fragmentation and the formation of Population III stars. Monthly Notices of the Royal Astronomical Society, 2015, 449, pp.77-87. 10.1093/mnras/stu2573 . insu-03644957

HAL Id: insu-03644957

https://insu.hal.science/insu-03644957v1

Submitted on 28 Apr 2022

HAL is a multi-disciplinary open access archive for the deposit and dissemination of scientific research documents, whether they are published or not. The documents may come from teaching and research institutions in France or abroad, or from public or private research centers.

L'archive ouverte pluridisciplinaire **HAL**, est destinée au dépôt et à la diffusion de documents scientifiques de niveau recherche, publiés ou non, émanant des établissements d'enseignement et de recherche français ou étrangers, des laboratoires publics ou privés.

Monthly Notices of the ROYAL ASTRONOMICAL SOCIETY

MNRAS **449,** 77–87 (2015) doi:10.1093/mnras/stu2573

Disc fragmentation and the formation of Population III stars

M. A. Latif[1]★ and D. R. G. Schleicher[2,3]

[1]*Institut d'Astrophysique, UMR 7095 CNRS, Universite Pierre et Marie Curie, 98bis Blvd Arago, F-75014 Paris, France*
[2]*Institut für Astrophysik, Georg-August-Universität, Friedrich-Hund-Platz 1, D-37077 Göttingen, Germany*
[3]*Scuola Normale Superiore, Piazza dei Cavalieri 7, I-56126 Pisa, Italy*

Accepted 2014 November 28. Received 2014 November 24; in original form 2014 October 31

ABSTRACT

Our understanding of Population III star formation is still in its infancy. They are formed in dark matter minihaloes of 10^5–10^6 $M_\odot$ at $z = 20$–30. Recent high-resolution cosmological simulations show that a protostellar disc forms as a consequence of gravitational collapse and fragments into multiple clumps. However, it is not entirely clear if these clumps will be able to survive to form multiple stars as simulations are unable to follow the disc evolution for longer times. In this study, we employ a simple analytical model to derive the properties of marginally stable steady-state discs. Our results show that the stability of the disc depends on the critical value of the viscous parameter α. For $\alpha_{\rm crit} = 1$, the disc is stable for an accretion rate of $\leq 10^{-3}$ $M_\odot$ yr^{-1} and becomes unstable at radii about $\geq$100 au in the presence of an accretion rate of 10^{-2} $M_\odot$ yr^{-1}. For $0.06 < \alpha_{\rm crit} < 1$, the disc can be unstable for both accretion rates. The comparison of the migration and the Kelvin–Helmholtz time-scales shows that clumps are expected to migrate inwards before reaching the main sequence. Furthermore, in the presence of a massive central star, the clumps within the central 1 au will be tidally disrupted. We also find that UV feedback from the central star is unable to disrupt the disc, and that photoevaporation becomes important only once the accretion rate has dropped to 2×10^{-4} $M_\odot$ yr^{-1}. As a result, the central star may reach a mass of 100 $M_\odot$ or even higher.

Key words: stars: formation – stars: Population III – galaxies: formation – cosmology: theory – early Universe.

1 INTRODUCTION

The first generation of stars, known as the Population III (Pop III) stars ushered the cosmos out of the dark ages and brought the first light. They reionized the universe via their stellar radiation and enriched the intergalactic medium with metals through supernova explosions. They further influenced the subsequent structure formation through their chemical, mechanical and radiative feedback (Bromm 2004; Ciardi & Ferrara 2005; Schleicher, Banerjee & Klessen 2008; Greif 2014). Hence, their comprehension is a matter of prime astrophysical interest and intrinsically linked to the understanding of key epochs in the universe.

According to the hierarchical paradigm of structure formation, Pop III stars are assembled in primordial dark matter haloes of 10^5–10^6 $M_\odot$ at $z = 20$–30. The gas falls into the dark matter potential and gets heated up to the virial temperature of the halo (i.e. ∼2000 K). In the absence of metals, H_2 is the only coolant which can bring the temperature down to a few hundred K and induce star formation. The trace amount of molecular hydrogen formed via gas-phase reactions gets boosted during the process of virialization and triggers the collapse in minihaloes. At high densities (10^8 cm^{-3}), the three-body reactions turn the gas into a fully molecular state and finally the gas becomes optically thick to molecular hydrogen cooling above 10^{18} cm^{-3}. At this stage, the thermal evolution becomes adiabatic and the birth of the Pop III stars takes place (Omukai 2000; Yoshida et al. 2006).

The first numerical simulations performed to study the formation of Pop III stars showed that they had masses of about a few hundred solar and were living isolatory lives (Abel, Bryan & Norman 2000, 2002; Bromm, Coppi & Larson 2002; Yoshida et al. 2006). However, cosmological simulations performed during the past few years have improved the modelling of chemical processes and employed higher resolution below the au scales (Turk, Abel & O'Shea 2009; Clark et al. 2011; Greif et al. 2012; Bovino et al. 2013; Latif et al. 2013b; Hartwig et al. 2015). These studies show that a protostellar disc forms as a consequence of gravitational collapse and becomes unstable in the presence of higher accretion rates of about 10^{-2}–10^{-3} $M_\odot$ yr^{-1}. Consequently, multiple stars are expected to form per halo. These works have tremendously enhanced our understanding of primordial star formation. They are however unable to follow the collapse for longer time-scales due to the computational constraints. Hence, it is not clear if these secondary fragments can survive to form stars or get merged with the central star. Recently, further attempts have been made to include the stellar UV feedback from the central star (Hosokawa et al. 2011; Stacy, Greif & Bromm

★ E-mail: latif@iap.fr

© 2015 The Authors
Published by Oxford University Press on behalf of the Royal Astronomical Society

Downloaded from https://academic.oup.com/mnras/article/449/1/77/1295011 by guest on 28 April 2022

2012; Hirano et al. 2014; Susa, Hasegawa & Tominaga 2014) and to derive the initial mass function. These studies either include an approximate treatment of stellar feedback or allow only a single star per halo.

Motivated by the above-mentioned results, we derive the properties of a marginally unstable protostellar disc and the fate of the clumps formed via gravitational instabilities. To achieve this goal, we employ an analytical model to compute the expected masses of the clumps and the disc under various conditions. We further show how the chemical processes influence the stability of the disc and explore the potential impact of the stellar feedback. This study provides insight into the disc fragmentation and ultimately the masses of the first stars.

This paper is organized in the following way. In Section 2, we describe in detail our analytical model and assumptions behind it. We present our results in Section 3. In Section 3.1, we discuss the disc properties for the disc mass dominated case where most of mass lies inside the disc at initial stage. In Section 3.2, we discuss the disc fragmentation in the presence of central star of various masses. In Section 3.3, we discuss the dependence of our results on the critical value of the viscous parameter α. In Section 3.4, we discuss the potential impact of UV feedback from the central star. In Section 4, we summarize our findings and discuss the caveats in our model.

2 MODEL

Our model is mainly based on Inayoshi & Haiman (2014). We consider the properties of a protostellar disc forming in a minihalo of 10^5–10^6 $M_\odot$ at $z = 25$. The disc is metal-free, composed of a primordial gas composition, fully molecular and predominantly cooled by the molecular hydrogen. The typical accretion rates on to such a disc are expected to be in the range of 10^{-2}–10^{-4} $M_\odot$ yr^{-1} as found from numerical simulations (Latif et al. 2013b). The main difference between our current study and Inayoshi & Haiman (2014) is that they studied the fragmentation of the disc forming in the massive primordial halo of $\sim 10^8$ $M_\odot$ mainly cooled by atomic line cooling. Particularly, they investigated the impact of H^- cooling occurring at high densities which induces fragmentation in the inner part of the disc, while we focus on the disc forming around Pop III star in minihalo cooled by molecular hydrogen.

To study the fragmentation of a self-gravitating protostellar accretion disc, we assume that it is in a steady-state condition. The stability of the disc can be measured from the Toomre parameter Q which is defined as

$$Q = \frac{c_s \Omega}{\pi G \Sigma}, \tag{1}$$

where Ω is the orbital frequency, c_s is the sound speed, G is the gravitational constant and Σ the surface density of the disc given as

$$\Sigma = \frac{\dot{M}_{tot}}{3\pi\nu}, \tag{2}$$

where $\dot{M}_{tot}$ is the mass accretion rate. We consider here the cases with $\dot{M}_{tot} = 10^{-2}$ and 10^{-3} $M_\odot$ yr^{-1}. ν is the viscosity in the disc arising from gravitational torques. The disc is presumed to be marginally stable with Toomre $Q = 1$. The scaleheight of the disc is computed assuming hydrostatic equilibrium in the vertical direction

$$H = \frac{c_s}{\Omega} \tag{3}$$

and the particle density is defined as

$$n = \frac{\Sigma}{4 m_p H}, \tag{4}$$

where m_p is the proton mass. The thermal state of the disc can be obtained by assuming thermal equilibrium, i.e. the heating rate (Q_+) is equivalent to cooling rate (Q_-). The main source of heating in the disc is the viscous heating by turbulence and shocks which can be computed as (Lodato 2007)

$$Q_+ = \frac{9}{4}\nu\Sigma\Omega^2 \tag{5}$$

and cooling rate is given by

$$Q_- = 2H\Lambda_{H_2/CIE}, \tag{6}$$

where $\Lambda_{H_2/CIE}$ is the net cooling rate in units of erg cm^{-3} s^{-1} and H is the height of the disc. The H_2 line cooling becomes optically thick at densities above 10^8 cm^{-3} and is estimated in the following way:

$$\Lambda_{H_2} = \Lambda_{H_2,thin} f_{thick}, \tag{7}$$

where $\Lambda_{H_2,thin}$ is the optically thin H_2 line cooling rate and f_{thick} is the factor which takes into account the opacity corrections. The expression for f_{thick} is taken from Ripamonti & Abel (2004) and is given as $min[1, (n_{H_2}/(8 \times 10^9\ cm^{-3}))^{-0.45}]$. By solving the thermal balance with respect to Ω assuming gas in the disc is fully molecular, we get the following relation:

$$\Omega^2 = \frac{24\pi c_s}{9\dot{M}_{tot}} \frac{(8 \times 10^9)^{0.45}}{\sqrt{4\pi m_p G}} \Lambda_{H_2}. \tag{8}$$

For $H_{2,\,thin}$ cooling, we use the cooling function for high-density limit given in Galli & Palla (1998) originally computed by Hollenbach & McKee (1979). We take into account the cooling due to the collisional induced emission (CIE) from molecular hydrogen which becomes dominant coolant at densities above 10^{13} cm^{-3}, often referred as H_2 continuum cooling (Omukai 2000; Ripamonti & Abel 2004). The importance of CIE cooling has been investigated in detail in numerical simulations (Yoshida, Omukai & Hernquist 2008; Hirano & Yoshida 2013). They found that it influences the cloud morphology and may even induce fragmentation. For the regime dominated by CIE cooling, we get the following expression for Ω by solving the thermal balance:

$$\Omega = \frac{9\dot{M}_{tot}}{24\pi c_s} \frac{(4\pi m_p G)^2}{\Lambda_{CIE}}, \tag{9}$$

where Λ_{CIE} is the optically thin CIE cooling rate and we use the fit given in equation (17) of Grassi et al. (2014).

Our treatment for the CIE cooling is relatively simple and does not include radiative transfer effects. For a spherical collapse, at densities above 10^{16} cm^{-3} the gas starts to become optically thick to the CIE cooling. However, for the disc geometry, an optically thin approximation may be valid even up to higher densities. We therefore expect at most a minor correction due to the approximation employed here, which has however no influence on our main results. Additional contributions to the thermal evolution may come from the chemical heating and cooling due to the formation and dissociation of H_2, which is not included in our model. For a stationary disc, we assume here that also the chemical abundances have reached their equilibrium value, and that no further chemical heating or cooling occurs. However, as simulations show (Omukai 2000; Bovino et al. 2013; Latif et al. 2013b), these processes can be relevant at earlier stages or at the transition point between different regimes.

Downloaded from https://academic.oup.com/mnras/article/449/1/77/1295011 by guest on 28 April 2022

For a viscous disc, we use the standard description for α by Shakura & Sunyaev (1973) and is given as

$$\nu = \alpha c_s H. \tag{10}$$

The properties of the fragmenting disc are computed based on above equations. The viscous parameter α can be computed by combing equations (1), (2), (3) and (10) as

$$\alpha = \frac{\dot{M}_{\rm tot} G}{3 c_s^3}. \tag{11}$$

The disc becomes unstable for $\alpha > \alpha_{\rm crit}$ (Gammie 2001). The initial masses of clumps can be estimated as follows:

$$M_{\rm c,i} = \Sigma H^2. \tag{12}$$

The clumps in the disc grow via accretion. The maximum clump mass so-called the gap-opening mass is computed by using the relation given in Levin (2007):

$$M_{\rm c} = M_{\rm c,i} \left[12\pi \frac{\alpha}{0.3}\right]^{1/2} \left(\frac{R}{H}\right)^{1/2}, \tag{13}$$

where R is the radius of the disc. The Kelvin–Helmholtz (KH) contraction time-scale estimated in Inayoshi & Haiman (2014) is equivalent to the mass accretion time-scale and allows us to estimate the duration of the adiabatic phase of protostellar evolution. Here, we instead consider the protostellar contraction phase, which is more relevant in the presence of lower accretion rates, it is computed as (Hosokawa, Omukai & Yorke 2012)

$$t_{\rm KH} = \frac{G M_*^2}{R_* L_*}, \tag{14}$$

where M_* is the mass, R_* is the radius and L_* is the luminosity of the protostar. We use equation (4) of Hosokawa et al. (2012) to compute the luminosity and their fig. 5 to estimate the radius of the star. The mass accretion rate on to the clumps and is defined as

$$\dot{M}_{\rm c} = \frac{3}{2} \Sigma \Omega \left(R_{\rm H}\right)^2, \tag{15}$$

where $R_{\rm H}$ is the Hill radius given as

$$R_{\rm H} = R \left(M_{\rm c}/30 M_*\right)^{1/3}, \tag{16}$$

where M_* is the mass of central star and is taken as 1 $M_\odot$. The migration time is considered to be equivalent to the viscous time-scale and is given as (Lin & Papaloizou 1986)

$$t_{\rm mig} = \frac{1}{3\pi\alpha} \left(\frac{R}{H}\right)^2 \frac{2\pi}{\Omega}. \tag{17}$$

This approximation is valid for the type-II migration in the theory of planet–disc interactions. The type-I migration time-scale is valid for low-mass planets when the perturbations induced by them are in the linear regime. It is even shorter than the type-II migration time-scale. So, our choice of the migration time-scale is rather conservative. We expect this time-scale to be shorter for the clumpy discs. The clumps can be further destroyed by the tidal forces exerted by central star. To estimate this effect, we compute the Roche limit which is given as

$$R_{\rm Roche} = 1.26 \times R_{\rm c} \left(M_*/M_{\rm c}\right)^{1/3}, \tag{18}$$

where $R_{\rm c}$, $M_{\rm c}$ are the radius and mass of the secondary clump and M_* is the mass of the central star.

2.1 Disc mass dominated case

In this subsection, we consider the early phase of the disc evolution where most of the mass lies within the disc. We study the disc structure and explore the fragmentation properties of the disc. In this case, the relation between the orbital frequency and radius obeys the following relation:

$$\Omega = \frac{2 c_s}{R}. \tag{19}$$

The surface density of the disc can be written as a function of orbital frequency:

$$\Sigma = \frac{\Omega c_s}{\pi G} \tag{20}$$

and the density inside the disc is

$$n = \frac{\Omega^2}{4\pi m_{\rm p} G}. \tag{21}$$

The rest of the quantities can be expressed in terms of radius by employing the relation given in equation (19).

2.2 Star mass dominated case

In the previous subsection, we assumed that the mass of the central star is negligible and that most of the mass lies within the disc. However, once a star is formed it will grow via rapid accretion and may change the disc structure. In this case, the mass of the central star exceeds the disc mass and modifies the relation between the orbital frequency and the disc radius. Assuming Kepler rotation, we have

$$R = \left(G M_*/\Omega^2\right)^{1/3}, \tag{22}$$

where M_* is the mass of the central star. The surface density of the disc can be computed as follows:

$$\Sigma = \frac{c_s}{\pi G} \sqrt{\frac{G M_*}{R^3}} \tag{23}$$

and the density inside the disc is

$$n = \frac{\Sigma}{4\pi m_{\rm p} c_s} \sqrt{\frac{G M_*}{R^3}}. \tag{24}$$

Similarly, the rest of the properties can be computed by replacing $\Omega = \sqrt{\frac{G M_*}{R^3}}$ in the equations given above.

3 RESULTS

We present our results in this section. In the following subsections, we describe the properties at the initial stage of the collapse where most of the mass lies inside the disc. We also consider the late stage of disc evolution when central star is formed and investigate how it changes the disc structure. The potential impact of the stellar UV feedback on the disc is explored in the last section.

3.1 The initial stage of fragmentation (disc dominated)

The properties of a marginally stable disc are computed by solving the set of equations presented in the previous section and are shown in Fig. 1. We consider here typical accretion rates of 10^{-2} $M_\odot$ yr^{-1} (hereafter called $\dot{M}_{-2}$) and 10^{-3} $M_\odot$ yr^{-1} (hereafter called $\dot{M}_{-3}$)

Downloaded from https://academic.oup.com/mnras/article/449/1/77/1295011 by guest on 28 April 2022

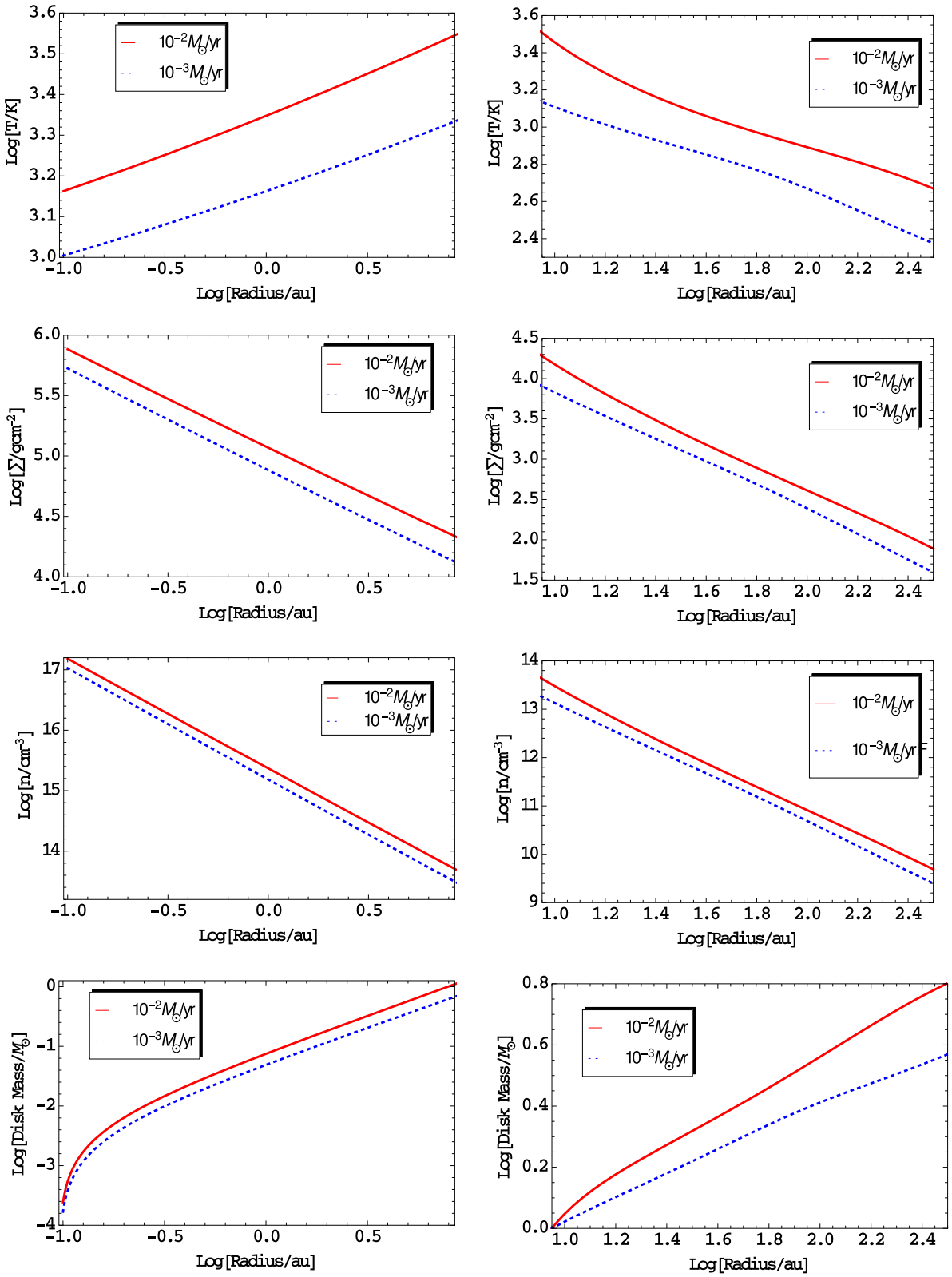

Figure 1. The properties of the disc are plotted against the radius for the disc mass dominated case. The red and blue lines represent accretion rates of 10^{-2} and 10^{-3} $M_{\odot}$ yr^{-1}, respectively. The left-hand panel shows the CIE cooling regime while the right-hand panel depicts H_2 cooling regime. The temperature, the density, the surface density and the enclosed mass in the disc are shown here.

Downloaded from https://academic.oup.com/mnras/article/449/1/77/1295011 by guest on 28 April 2022

often found in numerical simulations. For cooling, we consider optically thick H_2 line cooling between densities of 10^9 and 10^{14} cm^{-3} and above 10^{14} cm^{-3} cooling due to the CIE. These are the major cooling mechanisms in in these regimes. The thermal evolution of the disc is determined by solving the energy conservation equation ($Q_+ = Q_-$) and is shown against the disc radius. As the density inside the disc increases, H_2 line cooling becomes optically thick and the gas is heated up to 3100 K around 10 au while the temperature declines towards larger radii. The temperature of the disc at 300 au is about 400 K. It is found that the temperature of the disc is almost two times higher for $\dot{M}_{-2}$ compared to $\dot{M}_{-3}$. Towards smaller radii, the optically thick H_2 cooling becomes inefficient, and therefore other cooling channels need to be considered.

In particular, the CIE cooling becomes effective and reduces the disc temperature to about 1400 K for $\dot{M}_{-2}$ and 1000 K for $\dot{M}_{-3}$. The particle density in the disc varies from 10^{10} to 10^{14} cm^{-3} between 10 and 300 au and 10^{14} and 10^{17} cm^{-3} within the central 10 au. The density profile follows $R^{-1.5}$ in the inner 10 au and $R^{-2.6}$ between 10 and 300 au. The density is about a factor of 2 higher for $\dot{M}_{-2}$. The surface density is shallower within 0.1–10 au (10^4–5×10^5 g cm^{-2}) and becomes steeper between 10 and 300 au as it varies from 30 to 10^4 g cm^{-2}. The mass of the disc at a given radius is shown in the bottom panel of Fig. 1. The disc is about two times more massive for $\dot{M}_{-2}$ in comparison with $\dot{M}_{-3}$.

Motivated by the hydrodynamical simulations and analytical studies which show that the disc becomes unstable for $\alpha > \alpha_{\rm crit}$ (Gammie 2001; Rice, Lodato & Armitage 2005; Inayoshi & Haiman 2014), Zhu et al. (2012) investigated the fragmentation in a protoplanetary disc by performing numerical simulations and show that the disc becomes unstable for $\alpha > 1.0$. To measure the stability of the disc, we use $\alpha > 1.0$ in our model as a fragmentation criterion but also discuss below how this choice affects our results. We hereafter call this point the fragmentation radius. We have computed the value of α for the disc and it is shown in Fig. 2. The results from our model show that the value of α remains lower than 1 inside the central 10 au for both accretion rates. At larger radii, α remains lower than one for $\dot{M}_{-3}$ but becomes larger than one for $\dot{M}_{-2}$ around 100 au. Based on these results, it is expected that the disc remains stable for smaller accretion rates (i.e. $\dot{M}_{-3}$) and becomes unstable at larger radii for $\dot{M}_{-2}$. However, for $0.06 < \alpha_{\rm crit} < 1.0$ (see our discussion below), the disc becomes unstable and may even fragment at smaller radii. In fact, high-resolution simulations show fragmentation on scales of less than 1 au but it is not clear whether these clump will form stars as the simulations were evolved only for very short time-scales (Greif et al. 2012).

We have also estimated the masses of the clumps which are shown in Fig. 2. They have subsolar masses and are more massive in the outer parts of the disc than inside. The typical accretion rates on the clumps shown in Fig. 2 are about 10^{-3} M$_\odot$ yr^{-1} and about an order of magnitude higher for $\dot{M}_{-2}$. The clumps grow via accretion from the ambient medium and their masses are increased by an order of magnitude. The final masses of the clumps are shown in the bottom panel of Fig. 2. It is found that final clump masses in the outskirts of the disc reach about a solar mass for $\dot{M}_{-2}$. To know the fate of these clumps, we have computed their migration time and compared it with the KH contraction time-scale ($T_{\rm KH}$). The comparison is shown in Fig. 3, it is found that the migration time is shorter than the $T_{\rm KH}$. Therefore, clumps will migrate inward before they reach the main sequence and produce UV feedback.

3.2 Fragmentation in the presence of a central object (star dominated)

In the later stages of the disc evolution, it is expected that the potential from the central star starts to dominate and changes the disc structure. We have estimated the disc properties for a central star of 5, 50 and 500 solar masses. For the accretion rates considered here, the expected radii of these star are smaller than 100 R$_\odot$ (Hosokawa et al. 2012; Schleicher et al. 2013). Therefore, we do not show the scales smaller than this in our model for the star-dominated cases. It is found that in the presence of the central star, the disc becomes denser and hotter. Therefore, the CIE cooling kicks in earlier at larger radii as shown in Fig. 4. The density of 10^{17} cm^{-3} is already reached at 0.6 au where the gas start to become optically thick to CIE cooling which is not included in our model. However, we expect that at higher densities the temperature in the disc begins to evolve almost adiabatically. The value of the viscous parameter α remains lower than 1 for $\dot{M}_{-3}$ similar to the disc-dominated case. For $\dot{M}_{-2}$, the disc becomes unstable above 100 au and remains stable in the interior.

The masses of the clumps are similar to the disc-dominated cases both in the H_2 line and CIE cooling regimes. About solar mass clumps are expected to form between 100 and 300 au where the disc becomes unstable. We have also compared the migration and KH time-scales as shown in Fig. 5. It is found that the ratio of $T_{\rm mig}$ to $T_{\rm KH}$ remains close to one. It comes from the fact that in the star mass dominated case, the orbital period becomes shorter and the ratio of $T_{\rm KH}$ to $T_{\rm mig}$ declines.

We have also considered the cases with a central star of 50 and 500 solar masses. The disc becomes denser and warmer even at larger radii compared to the disc mass dominated case as shown in Figs 6 and 7. For the case of 50 solar mass central star and $\dot{M}_{-2}$, the fragmentation radius shifts further to larger radii of 300 au. The disc becomes completely stable for both accretion rates for the central star of 500 M$_\odot$. Moreover, the migration time-scale remains shorter than KH time-scale. Therefore, the clumps are expected to migrate inward. Our estimates for the Roche limit for the central star of 500 solar masses show that clumps will not be able to survive within the 1 au due to the tidal forces exerted by the central star.

3.3 Dependence on the critical value of alpha

So far we have assumed the value of $\alpha_{\rm crit} = 1$ as the criterion for the stability of the disc. This choice is motivated by the works of Zhu et al. (2012) and Inayoshi & Haiman (2014). However, the critical value of α can vary between 0.06 and 1. Rice et al. (2005) have suggested that the value of $\alpha_{\rm crit}$ is 0.06 although they did not have the realistic model for the heating and cooling of the disc. By considering the critical value of $\alpha = 0.06$, the disc in our model becomes unstable for both accretion rates and will fragment. Fig. 2 in Zhu et al. (2012) shows that in fact realistic cases may lie in between these extreme scenarios, so it is possible that fragmentation occurs for the value of α smaller than 1. Therefore, fragmentation may occur in the disc interior as found in high-resolution numerical simulations (Greif et al. 2012). Nevertheless, the ratio of $T_{\rm KH}$ to $T_{\rm mig}$ always remains ≥ 1. The clumps are expected to migrate inward before reaching the main sequence. Furthermore, they will be tidally disrupted in the central part of the disc depending on the mass of the central star. Therefore, we argue that the choice of the critical value of α does not change our main conclusions.

Downloaded from https://academic.oup.com/mnras/article/449/1/77/1295011 by guest on 28 April 2022

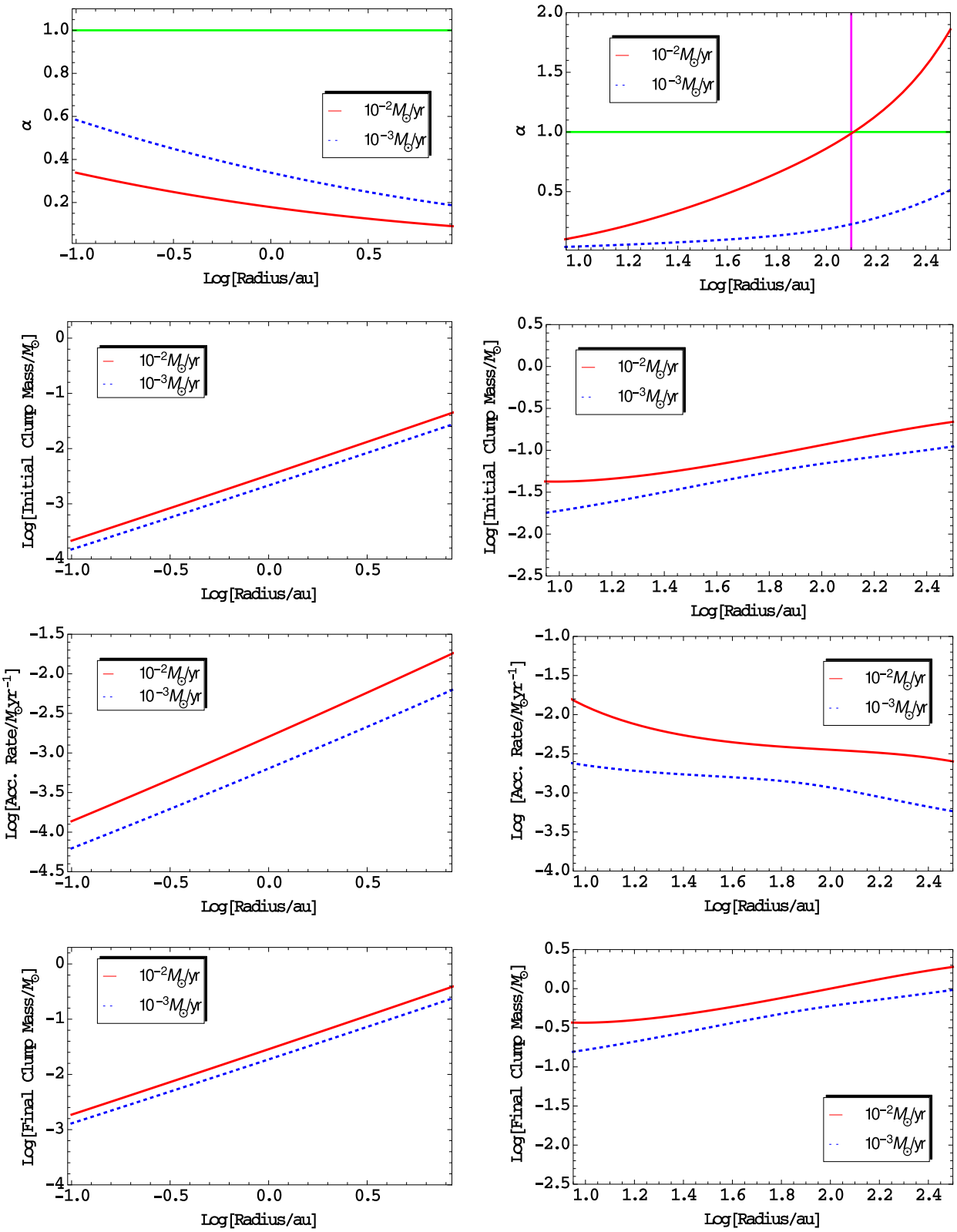

Figure 2. The properties of the disc are plotted against the radius for the disc mass dominated case. The red and blue lines represent accretion rates of 10^{-2} and 10^{-3} $M_\odot$ yr^{-1}, respectively. The left-hand panel shows the CIE cooling regime while the right-hand panel depicts H_2 cooling regime. The vertical magenta line shows the fragmentation radius and the horizontal green line marks the point where $\alpha = 1$. The viscous parameter α, the initial clump masses, accretion rates on to the clumps and their masses after the accretion are shown here.

Downloaded from https://academic.oup.com/mnras/article/449/1/77/1295011 by guest on 28 April 2022

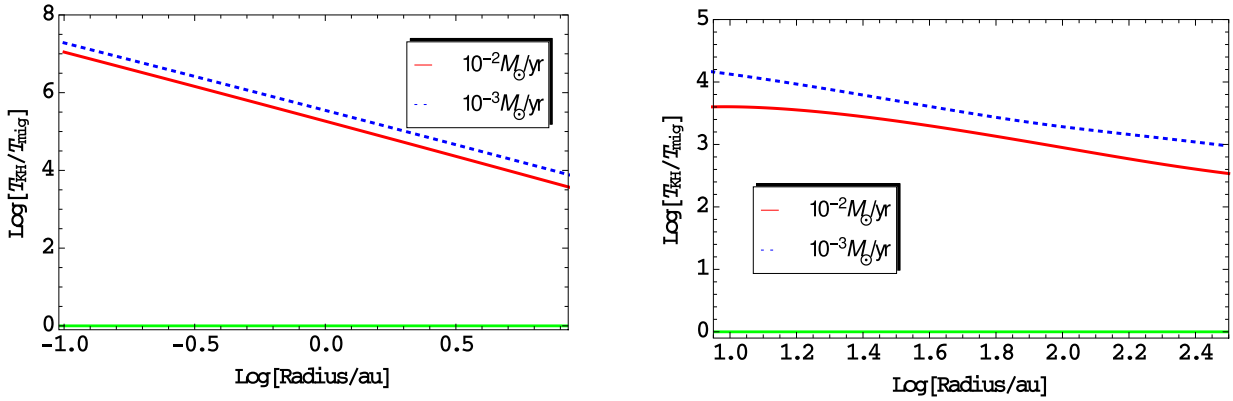

Figure 3. The ratio of the KH to the migration time-scales is shown here for the disc mass dominated case. The red and blue lines represent accretion rates of 10^{-2} and 10^{-3} $M_\odot$ yr^{-1}, respectively. The left-hand panel shows the CIE cooling regime while the right-hand panel depicts H_2 cooling regime.

3.4 Radiative feedback from the central object

Once the central star reaches the main sequence, it will start to produce UV flux which can photoionize the gas in the surroundings and photoevaporate the disc. The studies which consider the impact of stellar UV feedback on to the accretion flows through disc show that effect of UV starts to become important about 20 $M_\odot$ and photoevaporation shuts the accretion between 50 and 100 $M_\odot$ (McKee & Tan 2008; Hosokawa et al. 2011). However, the accretion from the disc may still continue. To compute the photoevaporation rate of the disc, we use the expression given in Hollenbach et al. (1994):

$$\dot{M}_{\rm PE} = 1.3 \times 10^{-5} \left(\frac{\phi_{\rm UV}}{10^{49}\,{\rm s}^{-1}}\right)^{1/2} \left(\frac{M_*}{10\,{\rm M}_\odot}\right)^{1/2} {\rm M}_\odot\,{\rm yr}^{-1}, \tag{25}$$

where $\phi_{\rm UV}$ is the photoionizing rate and M_* is the mass of a star. A star of 40 $M_\odot$ produces $\phi_{\rm UV} = 1.8 \times 10^{49}$ s^{-1} (Schaerer 2002). It gives the photoevaporation rate of 3.5×10^{-5} $M_\odot$ yr^{-1}. For a 500 $M_\odot$, $\phi_{\rm UV} = 5.2 \times 10^{50}$ s^{-1} which gives photoevaporation rate of 2.0×10^{-4} $M_\odot$ yr^{-1}. These are about an order of magnitude lower than the adopted mass accretion rates. Therefore, we expect that photoevaporation will not be able to completely terminate the accretion provided that such large accretion rates of the order of $\dot{M}_{-2}$ are maintained. However, Hosokawa et al. (2011) show that accretion rate declines down when star reaches above 40 solar masses. We expect that the latter is partly due to hydrodynamical effects and angular momentum conservation (see also Latif et al. 2013a), but also the UV feedback in the vertical direction, which decreases the mass supply on to the disc.

Recently Tanaka, Nakamoto & Omukai (2013) computed the photoevaporation rate from the disc by performing 2D asymmetric radiative transfer calculations and found that the photoevaporation rate depends on the disc radius instead of the gravitational radius. We also checked for the expression given in their equation (24) and found similar results.

To further assess the impact of photoionization, we compute the size of H II region by assuming the equilibrium between ionization and recombination. The equilibrium condition is given as

$$\dot{N} = \int_{R_{\rm i}}^{R_{\rm S}} 4\pi\alpha_{\rm rec} r^2 (n_0 (r/R)^l)^2 {\rm d}R, \tag{26}$$

where N is the photoionization rate, $R_{\rm S}$ is the radius of H II region, $R_{\rm i}$ is inner radius of the disc, n_0 is the corresponding density, $\alpha_{\rm rec}$ is the recombination rate for hydrogen and ℓ is the exponent of the density profile. Solving the above equation for $R_{\rm S}$, we get the following expression:

$$R_{\rm S} = \left(R_{\rm i}^{3-2l} + (3-2l)\frac{\dot{N}}{4\pi\alpha_{\rm rec} n_0^2 R^{2l}} \right)^{1/(3-2l)}. \tag{27}$$

Taking the numbers found in our model, $n_0 = 10^{17}$ cm^3, $\alpha_{\rm rec} = 3.0 \times 10^{-13}$ cm^3 s^{-1}, $R = 0.1$ au and $\ell = 1.6$ and $R_{\rm i} = 10\,R_\odot$. For a 40 solar mass star ($\dot{N} = 10^{49}$ s^{-1}), the size of H II region is 0.04 au. It is smaller than the scales probed in our model. We further expect that ionizing feedback from the central star of about 100 $M_\odot$ will not be able to strongly influence the disc structure. This result is further consistent with Hosokawa et al. (2011) who also found for a star >40 $M_\odot$ the H II region develops in the vertical direction and later on start to expand horizontally.

Our approach does not include the geometrical effects and assumes constant accretion rates. As found from the simulations, the declining accretion rates and the photoevaporation of the disc is expected to shut down the accretion above 100 solar masses.

4 DISCUSSION

We present here a simple analytical model to study the fragmentation properties of a marginally stable steady-state disc. Our model assumes that the Toomre $Q = 1$ and the disc is fully molecular. We solve the set of equations to compute the viscous parameter α. We check the stability of the disc by employing the fragmentation criterion based on recent numerical simulations which show that the disc becomes unstable for $\alpha > 1$. Our model includes a recipe for optically thick H_2 line cooling. We further take into account the CIE cooling occurring at high densities. The disc temperature is evaluated by assuming that heating by the turbulence viscosity and shocks is balanced by the cooling. The typical masses of the clumps are computed and their fate is determined by comparing the migration and contraction time-scales.

Our findings show that the temperature inside the disc increases for higher accretion rates and below 10 au, the CIE cooling becomes effective which brings the temperature down to about 1000 au. The densities in the disc range from 10^{10} to 10^{17} cm^{-3}. Our model shows that the stability of the disc depends on the critical value of the α. It remains stable for an accretion rate $\leq 10^{-3}$ $M_\odot$ yr^{-1} and becomes unstable at radii >100 au in the presence of higher accretion rate of 10^{-2} $M_\odot$ yr^{-1} for $\alpha > 1$. The typical masses of the clumps are about 0.1 $M_\odot$ and reach about solar masses in the regime where disc is unstable. For $\alpha_{\rm crit}$ between 0.06 and 1, the disc becomes

Downloaded from https://academic.oup.com/mnras/article/449/1/77/1295011 by guest on 28 April 2022

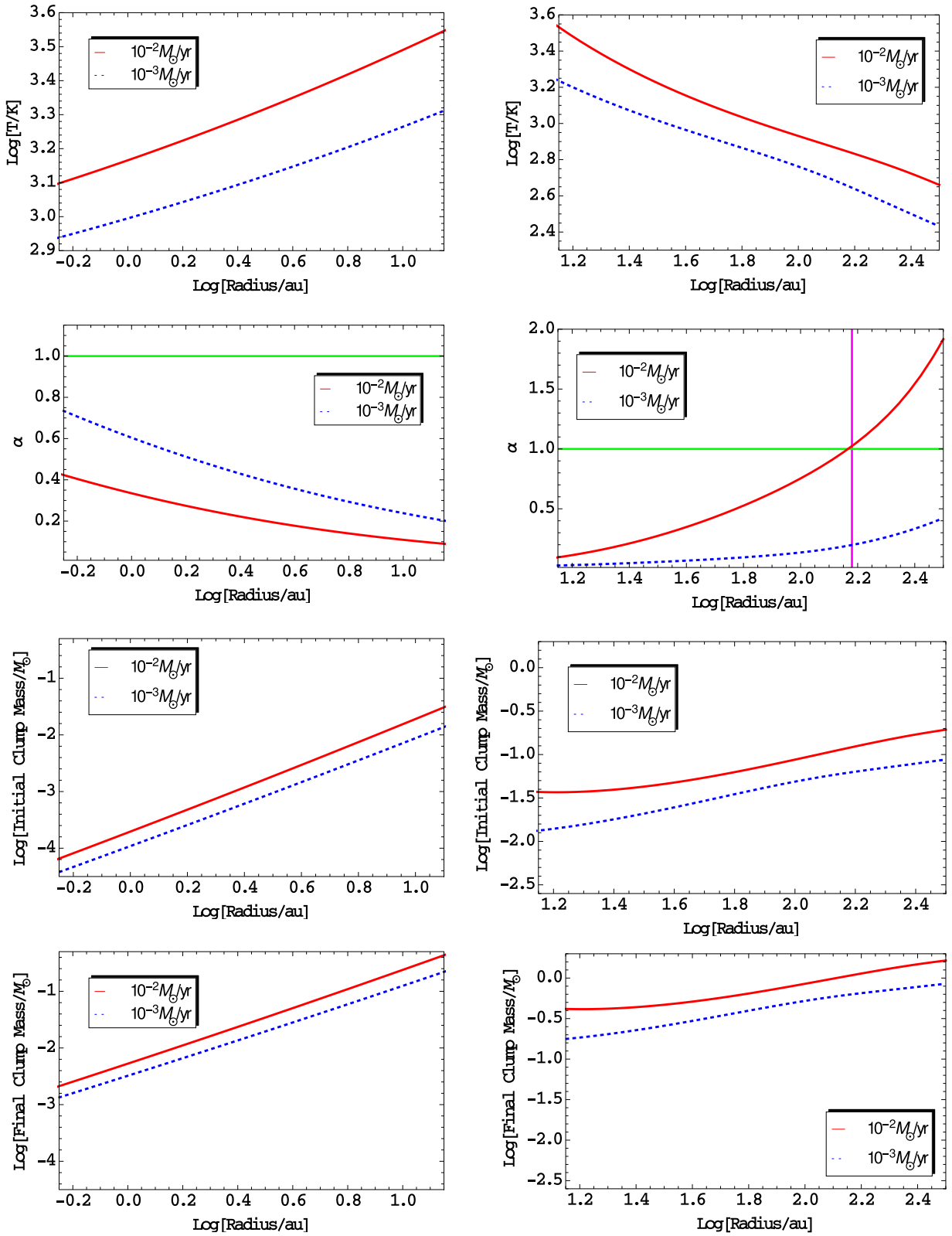

Figure 4. The properties of the disc are plotted against the radius for the central star of 5 solar masses. The red and blue lines represent accretion rates of 10^{-2} and 10^{-3} $M_{\odot}$ yr^{-1}, respectively. The vertical magenta line shows the fragmentation radius and the horizontal green line marks the point where $\alpha = 1$. The left-hand panel shows the CIE cooling regime while the right-hand panel depicts H_2 cooling regime. The temperature, the viscous parameter α, the clump masses before and after the accretion are shown here.

Downloaded from https://academic.oup.com/mnras/article/449/1/77/1295011 by guest on 28 April 2022

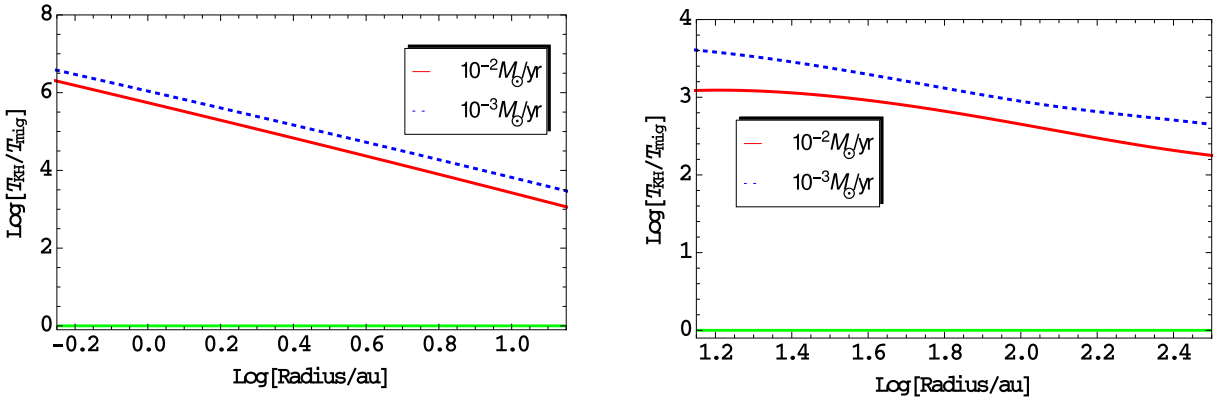

Figure 5. The ratio of the KH to the migration time-scales is shown for the central star of 5 solar masses. The red and blue lines represent accretion rates of 10^{-2} and 10^{-3} $M_\odot$ yr^{-1}, respectively. The left-hand panel shows the CIE cooling regime while the right-hand panel depicts H_2 cooling regime.

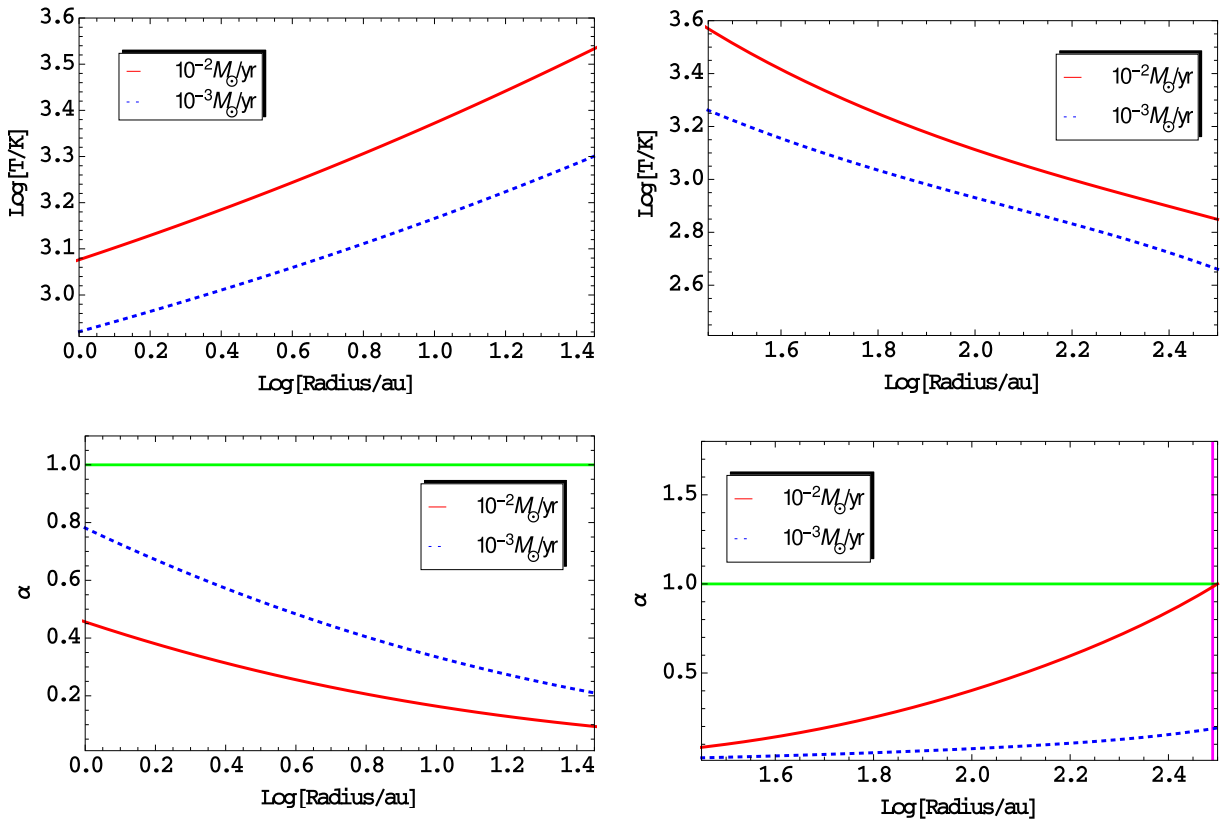

Figure 6. The temperature of the disc and the viscous parameter α are plotted against the radius for the central star of 50 solar masses. The red and blue lines represent accretion rates of 10^{-2} and 10^{-3} $M_\odot$ yr^{-1}, respectively. The vertical magenta line shows the fragmentation radius and the horizontal green line marks the point where α=1. The left-hand panel shows the CIE cooling regime while the right-hand panel depicts H_2 cooling regime.

unstable for both accretion rates. In this case, the disc is expected to fragment and form multiple clumps also on scales around 1 au as seen in high-resolution simulations (Greif et al. 2012). To compute the fate of the clumps, we compared the migration and the KH contraction time-scales. It is found that the clumps are migrated inwards and merge with the central star before reaching the main sequence. The clumps will be tidally disrupted within the central 1 au in the presence of a massive central star. So, the choice of the critical value $\alpha_{\rm crit}$ is not going to affect our main conclusions

We have also considered a few cases of the later disc phase when matter is accreted into the centre and a star is formed. In such a case, it dominates the central potential and changes the disc structure. We found that in the presence of a central star, the disc becomes denser and hotter. For a central star of 5 solar masses, the disc properties almost remain similar to the disc-dominated case. However, for a star of 50 and 500 $M_\odot$, the fragmentation radius shifts outwards and the disc becomes completely stable. Similar to the disc-dominated case, clumps are expected to migrate inwards and merge with central star. Our choice for the 50 and 500 $M_\odot$ stars comes from that fact that if accretion rates of 10^{-2} $M_\odot$ yr^{-1} are continued for 10 000 yr (the typical time before reaching the main sequence), then a massive star of the above-mentioned mass

Downloaded from https://academic.oup.com/mnras/article/449/1/77/1295011 by guest on 28 April 2022

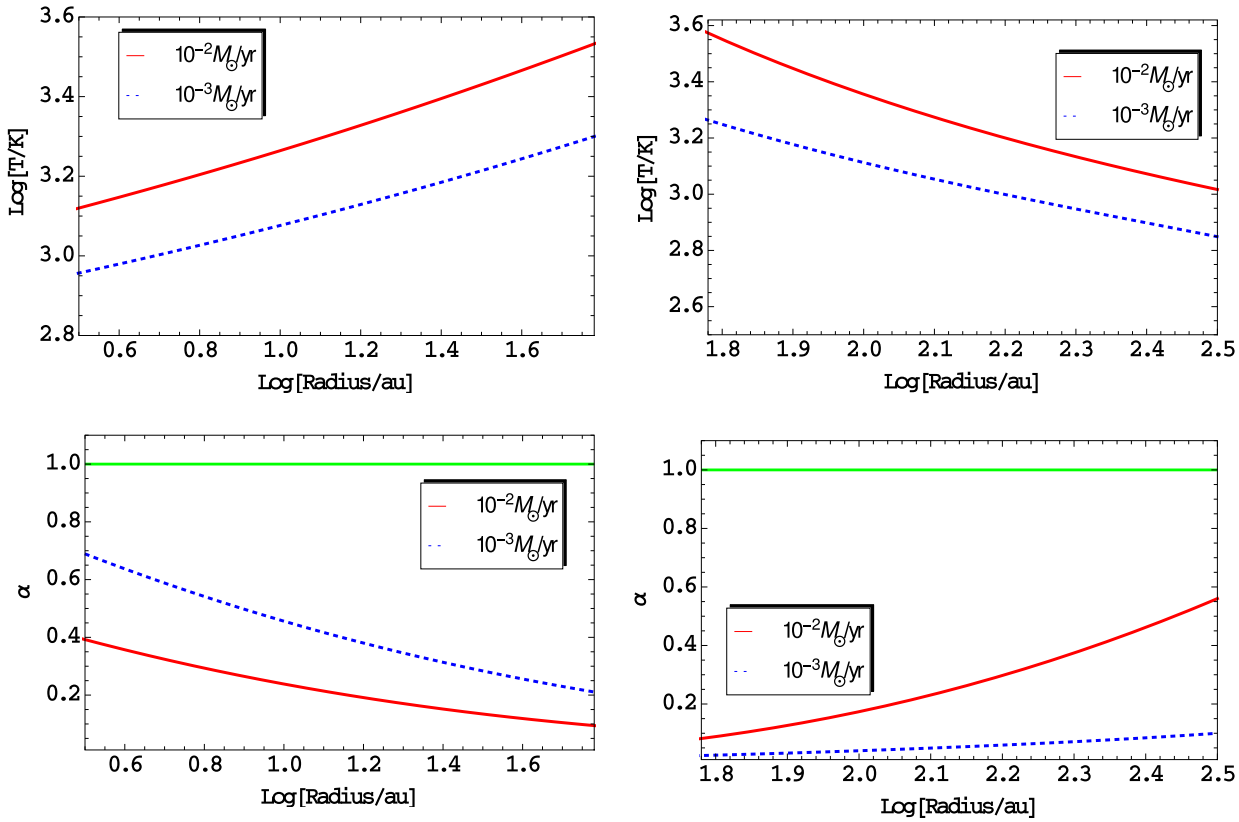

Figure 7. The temperature of the disc and the viscous parameter α are plotted against the radius for the central star of 500 solar masses. The red and blue lines represent accretion rates of 10^{-2} and 10^{-3} $M_\odot$ yr^{-1}, respectively. The horizontal green line shows the point where $\alpha = 1$. The left-hand panel shows the CIE cooling regime while the right-hand panel depicts H_2 cooling regime.

is expected to form. In fact, numerical simulations including the radiative feedback from the star show that such massive stars can form (Hirano et al. 2014; Susa et al. 2014).

We assumed constant accretion rates of 10^{-3} and 10^{-2} $M_\odot$ yr^{-1} on to the disc and found that in the presence of such accretion rates, the photoevaporation rate from the stellar UV feedback remains an order of magnitude lower. We therefore expect photoevaporation to become relevant once the accretion rate drops below $2 \times 10^{-4} M_\odot$ yr^{-1}. Similarly, we found that size of H II region remains smaller than 1 au and would not be able to completely disrupt the disc in equatorial plane. So, we expect that a star of about 100 $M_\odot$ may form. However, an H II region is likely to develop in the polar direction which will further expand with time as shown in numerical simulations (Hosokawa et al. 2011; Stacy et al. 2012). This may result in a decline of the accretion rates with time. McKee & Tan (2008) have estimated the impact of UV feedback from the star by including the radiation pressure and H_2 photodissociation rate. They also found that H II region develops in the polar direction for a 30 $M_\odot$ star which further expands beyond the gravitational radius between 50 and 100 solar masses. However, the accretion from the equatorial plane may continue. According to their estimates, above 140 solar masses, the combination of declining accretion rates and photoevaporation terminates the accretion.

We have studied the case where the disc is of a primordial composition which is valid for the discs around Pop III stars. However, the discs forming around the second generation of stars may already be polluted by the metals and dust ejected by the supernova explosions. The presence of trace amount of dust and metals may change the disc structure and make it unstable. Tanaka & Omukai (2014) have studied the disc fragmentation in various environments from zero to solar metallicity by employing an analytical model. They used an alternative approach by assuming that the viscous parameter $\alpha = 0.1$–1 and computed the Toomre Q. Their findings also show that the disc remains stable for the zero-metallicity case with $Q \geq 1$. However, for the lower metallicities, the disc becomes highly unstable. Therefore, masses of the stars in metal-polluted discs are expected to be much smaller.

We have assumed here that the disc is in a steady state but it may not always be the case. Our model is unable to capture 3D effects such as n-body interactions where some of these clumps may get ejected and eventually form stars. We have considered here the two different regimes of optically thick H_2 line cooling and H_2 CIE cooling. As a result, there is a minor discontinuity at the transition between these regimes. The latter will vanish in a realistic disc where the transition occurs more gradually. It has however no impact on our main results. To enhance our understanding of primordial star formation, we propose to pursue 3D simulations investigating the fragmentation properties of primordial discs at later stages of their evolution to quantify their fragmentation and migration behaviour.

ACKNOWLEDGEMENTS

We thank Marta Volonteri, Tilman Hartwig and Kazu Omukai for interesting discussions and helpful suggestions. The research leading to these results has received funding from the European Research Council under the European Community's Seventh Framework Programme (FP7/2007-2013 Grant Agreement No. 614199, project 'BLACK'). DRGS is indebted to the Scuola Normale

Downloaded from https://academic.oup.com/mnras/article/449/1/77/1295011 by guest on 28 April 2022

Superiore (SNS) in Pisa for an invitation as a 'Distinguished Scientist' which has stimulated the research described in this manuscript.

REFERENCES

Abel T., Bryan G. L., Norman M. L., 2000, ApJ, 540, 39
Abel T., Bryan G. L., Norman M. L., 2002, Science, 295, 93
Bovino S., Grassi T., Latif M. A., Schleicher D. R. G., 2013, MNRAS, 434, L36
Bromm V., 2004, PASP, 116, 103
Bromm V., Coppi P. S., Larson R. B., 2002, ApJ, 564, 23
Ciardi B., Ferrara A., 2005, Space Sci. Rev., 116, 625
Clark P. C., Glover S. C. O., Smith R. J., Greif T. H., Klessen R. S., Bromm V., 2011, Science, 331, 1040
Galli D., Palla F., 1998, A&A, 335, 403
Gammie C. F., 2001, ApJ, 553, 174
Grassi T., Bovino S., Schleicher D. R. G., Prieto J., Seifried D., Simoncini E., Gianturco F. A., 2014, MNRAS, 439, 2386
Greif T. H., 2014, preprint (arXiv:1410.3482)
Greif T. H., Bromm V., Clark P. C., Glover S. C. O., Smith R. J., Klessen R. S., Yoshida N., Springel V., 2012, MNRAS, 424, 399
Hartwig T., Clark P. C., Glover S. C. O., Klessen R. S., Sasaki M., 2015, ApJ, 799, 114
Hirano S., Yoshida N., 2013, ApJ, 763, 52
Hirano S., Hosokawa T., Yoshida N., Umeda H., Omukai K., Chiaki G., Yorke H. W., 2014, ApJ, 781, 60
Hollenbach D., McKee C. F., 1979, ApJS, 41, 555
Hollenbach D., Johnstone D., Lizano S., Shu F., 1994, ApJ, 428, 654
Hosokawa T., Omukai K., Yoshida N., Yorke H. W., 2011, Science, 334, 1250
Hosokawa T., Omukai K., Yorke H. W., 2012, ApJ, 756, 93
Inayoshi K., Haiman Z., 2014, MNRAS, 445, 1549
Latif M. A., Schleicher D. R. G., Schmidt W., Niemeyer J. C., 2013a, MNRAS, 436, 2989
Latif M. A., Schleicher D. R. G., Schmidt W., Niemeyer J., 2013b, ApJ, 772, L3
Levin Y., 2007, MNRAS, 374, 515
Lin D. N. C., Papaloizou J., 1986, ApJ, 309, 846
Lodato G., 2007, Nuovo Cimento Riv. Ser., 30, 293
McKee C. F., Tan J. C., 2008, ApJ, 681, 771
Omukai K., 2000, ApJ, 534, 809
Rice W. K. M., Lodato G., Armitage P. J., 2005, MNRAS, 364, L56
Ripamonti E., Abel T., 2004, MNRAS, 348, 1019
Schaerer D., 2002, A&A, 382, 28
Schleicher D. R. G., Banerjee R., Klessen R. S., 2008, Phys. Rev. D, 78, 083005
Schleicher D. R. G., Palla F., Ferrara A., Galli D., Latif M., 2013, A&A, 558, A59
Shakura N. I., Sunyaev R. A., 1973, A&A, 24, 337
Stacy A., Greif T. H., Bromm V., 2012, MNRAS, 422, 290
Susa H., Hasegawa K., Tominaga N., 2014, ApJ, 792, 32
Tanaka K. E. I., Omukai K., 2014, MNRAS, 439, 1884
Tanaka K. E. I., Nakamoto T., Omukai K., 2013, ApJ, 773, 155
Turk M. J., Abel T., O'Shea B., 2009, Science, 325, 601
Yoshida N., Omukai K., Hernquist L., Abel T., 2006, ApJ, 652, 6
Yoshida N., Omukai K., Hernquist L., 2008, Science, 321, 669
Zhu Z., Hartmann L., Nelson R. P., Gammie C. F., 2012, ApJ, 746, 110

This paper has been typeset from a TEX/LATEX file prepared by the author.

Downloaded from https://academic.oup.com/mnras/article/449/1/77/1295011 by guest on 28 April 2022